

Chirp Excitation

Navin Khaneja ^{*†}

May 16, 2017

Abstract

The paper describes the design of broadband chirp excitation pulses. We first develop a three stage model for understanding chirp excitation in NMR. We then show how a chirp π pulse can be used to refocus the phase of the chirp excitation pulse. The resulting magnetization still has some phase dispersion in it. We show how a combination of two chirp π pulses instead of one can be used to eliminate this dispersion, leaving behind a small residual phase dispersion. The excitation pulse sequence presented here allow exciting arbitrary large bandwidths without increasing the peak rf-amplitude. Experimental excitation profiles for the residual HDO signal in a sample of 99.5% D₂O are displayed as a function of resonance offset. Although methods presented in this paper have appeared elsewhere, we present complete analytical treatment that elucidates the working of these methods.

^{*}To whom correspondence may be addressed. Email:navinkhaneja@gmail.com

[†]Department of Electrical Engineering, IIT Bombay, Powai - 400076, India.

1 Introduction

The excitation pulse is ubiquitous in Fourier Transform-NMR, being the starting point of all experiments. With increasing field strengths in high resolution NMR, sensitivity and resolution comes with the challenge of uniformly exciting larger bandwidths. At a field of 1 GHz, the target bandwidth is 50 kHz for excitation of entire 200 ppm ^{13}C chemical shifts. The required 25 kHz hard pulse exceeds the capabilities of most ^{13}C probes and poses additional problems in phasing the spectra. In ^{19}F NMR, chemical shifts can range over 600 ppm, which requires excitation of different regions of the spectra. Methods that can achieve uniform excitation over the entire bandwidth in ^{19}F NMR, are therefore most desirable. Towards this end, several methods have been developed for broadband excitation/inversion, which have reduced the phase variation of the excited magnetization as a function of the resonance offset. These include composite pulses, adiabatic sequences, polycromatic sequences, phase alternating pulse sequences, optimal control pulse design, and method of multiple frames, [1]-[20].

In this paper, we develop the theory of broadband chirp excitation. We first develop a three stage model for understanding chirp excitation in NMR. We then show how a chirp π pulse can be used to refocus the phase of the excitation pulse. The resulting magnetization still has some phase dispersion in it. We show how a combination of two chirp π pulses instead of one can be used to eliminate this dispersion leaving behind a small residual phase dispersion. The pulse sequence presented here allow exciting arbitrary large bandwidths without increasing the peak rf-amplitude. Although methods presented in this paper have appeared elsewhere [7, 8, 18], we present complete analytical treatment that elucidates the working of these methods.

The paper is organized as follows. In section 2, we present the theory behind chirp excitation. In section 3, we present simulation and experimental results for broadband excitation pulses designed using chirp pulses. We conclude in section 4, with discussion and outlook.

2 Theory

Let

$$\Omega_x = \begin{bmatrix} 0 & 0 & 0 \\ 0 & 0 & -1 \\ 0 & 1 & 0 \end{bmatrix}, \quad \Omega_y = \begin{bmatrix} 0 & 0 & 1 \\ 0 & 0 & 0 \\ -1 & 0 & 0 \end{bmatrix}, \quad \Omega_z = \begin{bmatrix} 0 & -1 & 0 \\ 1 & 0 & 0 \\ 0 & 0 & 0 \end{bmatrix}.$$

denote generator of rotations around x, y, z axis respectively. A x -rotation by flip angle θ is $\exp(\theta\Omega_x)$.

A chirp excitation pulse is understood as concatenation of three rotations

$$\underbrace{\exp(\theta_0\Omega_y)}_{III} \underbrace{\exp(\alpha\Omega_x)}_{II} \underbrace{\exp(\theta_0\Omega_y)}_I$$

which satisfy

$$\cos \alpha = \tan^2 \theta_0.$$

Given the Bloch equation,

$$\dot{X} = (\omega_0\Omega_z + A \cos \phi \Omega_x + A \sin \phi \Omega_y)X,$$

where X is the magnetization vector,

The chirp pulse has instantaneous frequency $\dot{\phi} = \omega_c = -C + at$ where a is the sweep rate and phase $\phi(t) = -Ct + \frac{at^2}{2}$. The frequency ω_c is swept from $[-C, C]$, in time $T = \frac{2C}{a}$ with offsets in range $[-B, B]$.

In the interaction frame of the chirp phase, $\phi(t)$, we have $Y(t) = \exp(-\phi(t)\Omega_x)X(t)$, evolve as

$$\dot{Y} = ((\omega_0 - \omega_c)\Omega_z + A\Omega_x)Y = \tilde{\omega} (\cos \theta(t) \Omega_z + \sin \theta(t) \Omega_y)Y,$$

where effective field strength $\tilde{\omega} = \sqrt{(\omega_0 - \omega_c(t))^2 + A^2}$ and $\tan \theta(t) = \frac{A}{\omega_0 - \omega_c(t)}$.

The three stages of the chirp excitation are understood in this frame.

The first rotation, I , arises as frequency of the chirp pulse ω_c is swept from a large negative offset $-C$ to $\omega_c - \omega_0 = -A \cot \theta_0$. As a result, the initial magnetization follows the effective field and is transferred to

$$\begin{bmatrix} 0 \\ 0 \\ 1 \end{bmatrix} \rightarrow \begin{bmatrix} \sin \theta_0 \\ 0 \\ \cos \theta_0 \end{bmatrix}.$$

During the phase II of the pulse the frequency $\omega_c - \omega_0$ is swept over the range $[-A \cot \theta_0, A \cot \theta_0]$ in time $\frac{\alpha}{A}$ and for $\cot \theta_0$ not very larger than 1, we can approximate the evolution in this phase II as

$$\sim \exp\left(\int_0^{\alpha/A} (\omega_0 - \omega_c) \Omega_z + A \Omega_x\right) = \exp(\alpha \Omega_x).$$

This produces the evolution

$$\begin{bmatrix} \sin \theta_0 \\ 0 \\ \cos \theta_0 \end{bmatrix} \rightarrow \begin{bmatrix} \sin \theta_0 \\ -\cos \theta_0 \sin \alpha \\ \cos \theta_0 \cos \alpha \end{bmatrix}.$$

Finally, during phase III , the frequency is swept from $A \cot \theta_0$ to a large positive offset C in time t_f . This produces the transformation

$$\exp\left(-\underbrace{\int \tilde{\omega}(t) dt}_{\Phi(\omega_0)} \Omega_z\right) \exp(\theta_0 \Omega_y) \begin{bmatrix} \sin \theta_0 \\ -\cos \theta_0 \sin \alpha \\ \cos \theta_0 \cos \alpha \end{bmatrix}. \quad (1)$$

To see this, observe, given

$$\dot{Y} = \tilde{\omega} (\cos \theta \Omega_z + \sin \theta \Omega_y) Y,$$

in the interaction frame of θ where $Z = \exp(-\theta(t)\Omega_y)Y$, we have,

$$\dot{Z} = (\tilde{\omega}\Omega_z - \dot{\theta}\Omega_y)Z.$$

If $\tilde{\omega} \gg \dot{\theta}$, which is true in phase III of the pulse, where $a \ll \tilde{\omega}^2$, as will be shown below. Then in the interaction frame of $W = \exp(-\int_0^t \tilde{\omega}(t) \Omega_z)Z$, we average $W(t)$ to I . Therefore the evolution of the Bloch equation for the chirp pulse takes the form

$$\begin{aligned} Y(t_f) &= \exp(\theta(t_f)\Omega_y)Z(t_f) \\ &= \exp(\theta(t_f)\Omega_y) \exp\left(\int_0^{t_f} \tilde{\omega} \Omega_z\right) \underbrace{\exp(-\theta(0)\Omega_y) Y(0)}_{Z_0} \\ Y(t_f) &= \exp(\pi \Omega_y) \exp\left(\underbrace{\int_0^{t_f} \tilde{\omega} \Omega_z}_{\Phi(\omega_0)}\right) \exp(-\theta(0)\Omega_y)Y(0) \end{aligned} \quad (2)$$

where 0 marks beginning of phase III and $\theta(0) = \pi - \theta_0$, and $\theta(t_f) = \pi$. See Fig. 1 left panel. Then this gives Eq. (1).

Now for this to be an excitation, the z coordinate should vanish, which means,

$$\frac{\cos \theta_0 \cos \alpha}{\sin \theta_0} = \tan \theta_0. \quad (3)$$

$$\tan^2 \theta_0 = \cos \alpha. \quad (4)$$

For example, when $\cot^2 \theta_0 = 2$, we have $\cos \alpha = \frac{1}{2}$, i.e, $\alpha = 1.0472$. Thus phase *II* is traversed in time $\alpha A^{-1} = 1.0472 A^{-1}$. The frequency swept in this time is $2A \cot \theta_0 = 2A\sqrt{2}$. The sweep rate is $a = A^2 \frac{2\sqrt{2}}{1.0472} = 2.7A^2$. The smallest effective field in phase *I* and *III* is $\tilde{\omega}^2 = A^2(1 + \cot^2 \theta_0) = 3A^2$ in phase *I* and *III*. Therefore, in phase *I* and *III*, we have $a \leq \tilde{\omega}^2$ and adiabatic approximation is valid. In nutshell sweep rate $a = 2.7A^2$.

For another example, when $\cot^2 \theta_0 = 3$, we have $\cos \alpha = \frac{1}{3}$, i.e, $\alpha = 1.23$. Thus phase *II* is traversed in time $\alpha A^{-1} = 1.23 A^{-1}$. The frequency swept in this time is

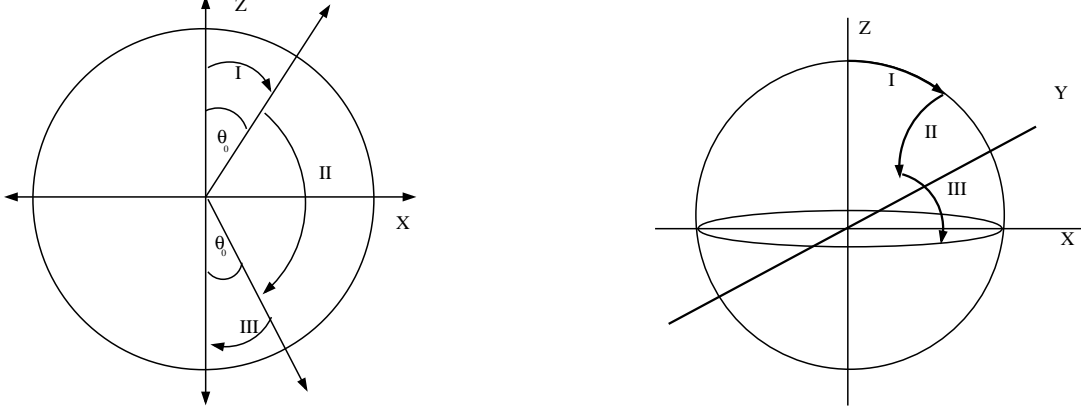


Figure 1: The left panel shows the effective field for the chirp excitation. The effective field starts along z axis and after phase I is rotated by θ_0 . After phase II, it makes angle of θ_0 with $-z$ axis and finally at end of phase III ends up at the $-z$ axis. The right panel shows how magnetization initially along z axis evolves in three stages. It is rotated along y axis in phase I by angle θ_0 and then along x axis by angle α in phase II and finally along y axis by θ_0 in phase III.

$2A \cot \theta_0 = 2A\sqrt{3}$. The sweep rate is $a = A^2 \frac{2\sqrt{3}}{1.23} = 2.81A^2$. The smallest effective field in phase I and III is $\tilde{\omega}^2 = A^2(1 + \cot^2 \theta_0) = 4A^2$ in phase I and III. Therefore, in phase I and III, we have $a \leq \tilde{\omega}^2$ and adiabatic approximation is valid.

In remaining paper we take $a = 2.7A^2$. The chirp excitation doesn't produce a uniform excitation phase for all offsets.

To understand this refer to Figure 2, where offsets vary from $[-B, B]$ and we sweep from $[-C, C]$ at rate a . It takes T_0 units of time to sweep from $-C$ to $-B$ and T_1 units of time to sweep from $-B$ to C . Let $T = T_0 + T_1$ be total time. It takes t_1 units of time to sweep from $\omega_c(t) - \omega_0 = 0$ to $\omega_c(t) - \omega_0 = A \cot \theta_0$. Then the phase Φ accumulated in Eq. 1 for the offset $-B$ is $\Phi(-B) = \int_{t_1}^{T_1} \tilde{\omega}(t) dt$ and for offset $-B + \Delta\omega = -B + a\Delta$ is $\Phi(-B + a\Delta) = \int_{t_1}^{T_1 - \Delta} \tilde{\omega}(t) dt$. The difference of the phases is

$$\int_{T_1 - \Delta}^{T_1} \tilde{\omega}(t) dt \sim \int_{T_1 - \Delta}^{T_1} \left(at + \frac{A^2}{2at} \right) dt = \frac{a}{2}(T_1^2 - (T_1 - \Delta)^2) + \frac{A^2}{2a} \ln \frac{T_1}{T_1 - \Delta}. \quad (5)$$

$$= \frac{a}{2}(-\Delta^2 + 2T_1\Delta) + \frac{A^2}{2a} \ln \frac{T_1}{T_1 - \Delta}. \quad (6)$$

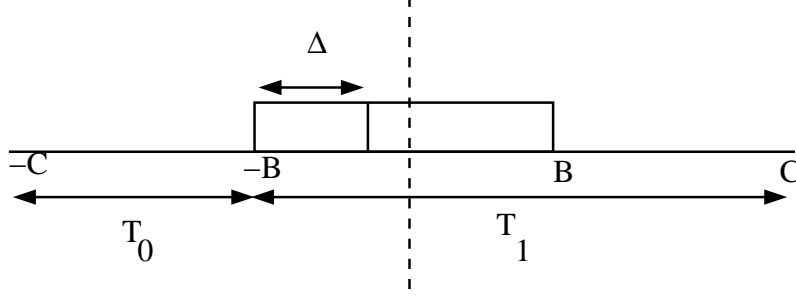


Figure 2: The figure shows the offsets in range $[-B, B]$ and the sweep of chirp from $[-C, C]$. T_1 is the time it takes to sweep from $-B$ to C and T_0 is the time to sweep from $-C$ to $-B$. Also shown is a offset that takes Δ time to reach from $-B$, at sweep rate a .

We can refocus this phase by following the chirp excitation pulse with a chirp π pulse at twice the sweep rate $a_1 = 2a$ and rf-field strength $A_1^2 \gg a_1$. To understand this, consider again the Bloch equation

$$\dot{X} = (\omega_0 \Omega_z + A_1 \cos \phi \Omega_x + A_1 \sin \phi \Omega_y)X,$$

where the chirp frequency $\dot{\phi} = \omega_c = -C + a_1 t$ is swept from $[-C, C]$.

In the interaction field of the chirp phase, $\phi(t)$, we have $Y(t) = \exp(-\phi(t)\Omega_x)X(t)$, and

$$\dot{Y} = ((\omega_0 - \omega_c)\Omega_z + A_1 \Omega_x)Y = \tilde{\omega} (\cos \theta \Omega_z + \sin \theta \Omega_y)Y,$$

where effective field strength $\tilde{\omega} = \sqrt{(\omega_0 - \omega_c(t))^2 + A_1^2}$ and $\tan \theta = \frac{A_1}{\omega_0 - \omega_c}$.

Now in interaction frame of θ where $Z = \exp(-\theta(t)\Omega_y)Y$, we have

$$\dot{Z} = (\tilde{\omega} \Omega_z - \dot{\theta} \Omega_y)Z.$$

If $\tilde{\omega} \gg \dot{\theta}$, which is true when rf-field strength $A_1^2 \gg a_1$, in the interaction frame of $W = \exp(-\int_0^t \tilde{\omega} \Omega_z)Z$, we average $W(t)$ to I . Therefore the evolution of the Bloch

equation for the chirp pulse takes the form

$$X(t) = \exp(\phi(t) \Omega_z) \exp(\theta(t) \Omega_y) \exp(\underbrace{\int_0^t \tilde{\omega} \Omega_z}_{\Phi_1(\omega_0)}) X(0) \quad (7)$$

where $\phi(0) = \phi(T) = 0$ and $\theta(0) = 0$ and $\theta(T) = \pi$ and now we can again evaluate $\Phi_1(-B) - \Phi_1(-B + a\Delta)$. Observe

$$\begin{aligned} \Phi_1(-B) &= \int_0^{\frac{T_0}{2}} \sqrt{(a_1 t)^2 + A_1^2} dt + \int_0^{\frac{T_1}{2}} \sqrt{(a_1 t)^2 + A_1^2} dt. \\ \Phi_1(-B + a\Delta) &= \int_0^{\frac{T_0+\Delta}{2}} \sqrt{(a_1 t)^2 + A_1^2} dt + \int_0^{\frac{T_1-\Delta}{2}} \sqrt{(a_1 t)^2 + A_1^2} dt. \\ \Phi_1(-B) - \Phi_1(-B + a\Delta) &= \int_{\frac{T_1-\Delta}{2}}^{\frac{T_1}{2}} \sqrt{(a_1 t)^2 + A_1^2} dt - \int_{\frac{T_0}{2}}^{\frac{T_0+\Delta}{2}} \sqrt{(a_1 t)^2 + A_1^2} dt. \\ \int_{\frac{T_1-\Delta}{2}}^{\frac{T_1}{2}} \sqrt{(a_1 t)^2 + A_1^2} dt &\sim \frac{a}{4}(T_1^2 - (T_1 - \Delta)^2) + \frac{A_1^2}{4a} \ln \frac{T_1}{T_1 - \Delta}. \\ \Phi_1(-B) - \Phi_1(-B + a\Delta) &\sim \frac{a}{4}(-2\Delta^2 + 2(T_1 - T_0)\Delta) + \frac{A_1^2}{4a} \ln \frac{T_1 T_0}{(T_1 - \Delta)(T_0 + \Delta)}. \end{aligned}$$

Now if we combine the phase due to chirp excitation excitation pulse and the chirp π pulse we get

$$\begin{aligned} \{\Phi_1(-B + a\Delta) - \Phi_1(-B)\} - \{\Phi(-B + a\Delta) - \Phi(-B)\} &= \frac{a(T_1 + T_0)\Delta}{2} - \frac{A_1^2}{4a} \ln \frac{T_1 T_0}{(T_1 - \Delta)(T_0 + \Delta)} \\ &+ \frac{A^2}{2a} \ln \frac{T_1}{T_1 - \Delta}. \end{aligned}$$

If chirp π pulse is followed by free evolution for $\frac{T}{2}$ where $T = T_1 + T_0$, it refocuses the phase $\frac{a(T_1+T_0)\Delta}{2} = \frac{T\Delta\omega}{2}$. See Fig. 3A. The only phase dispersion that is left is

$$\frac{A_1^2}{4a} \ln \frac{(T_1 - \Delta)(T_0 + \Delta)}{T_1 T_0} + \frac{A^2}{2a} \ln \frac{T_1}{T_1 - \Delta} \quad (8)$$

For $a\Delta = 2B$, the other extreme of the spectrum, the above expression simplifies to

$$\frac{A^2}{2a} \ln \frac{1 + \frac{B}{C}}{1 - \frac{B}{C}}. \quad (9)$$

As described before for $a = 2.7A^2$ and when $\frac{B}{C} \ll 1$ say $\frac{B}{C} = 1/3$, this dispersion is small around 7° .

The factor $\frac{A_1^2}{4a} \ln \frac{(T_1 - \Delta)(T_0 + \Delta)}{T_1 T_0}$ in Eq. (8) can be cancelled by introducing a π pulse of amplitude $\frac{A_1}{\sqrt{2}}$, and sweep rate a , following $\frac{\pi}{2}$ chirp pulse and then a delay of $\frac{T}{2}$, and finally the π pulse of amplitude A_1 and sweep rate $2a$. See Fig. 3B. Then all phase dispersion cancel except the one in Eq. (9). We can make this dispersion small by $\frac{B}{C} \ll 1$.

3 Simulation and Experiments

In Fig. 3A, we choose amplitude of π pulse as 10 kHz and $\frac{\pi}{2}$ pulse as 1 kHz. The bandwidth $B/2\pi = 50$ kHz and $C/2\pi = 400$ kHz. Sweep rate $a = (2\pi \text{ kHz})^2$ and time $T = 47.15$ ms. Total duration of the pulse is 94.13 ms. Fig. 4A, shows the x-coordinate of the excited magnetization, after a zero order phase correction.

In Fig. 3B, we choose amplitude of last π pulse as 10 kHz, center π pulse as $\frac{10}{\sqrt{2}}$ kHz and $\frac{\pi}{2}$ pulse as 1 kHz. The bandwidth $B/2\pi = 50$ kHz and $C/2\pi = 150$ kHz. Sweep rate $a = (2\pi \text{ kHz})^2$ and time $T = 17.68$ ms. Total duration of the pulse is 53.0516 ms. Fig. 4B, shows the x-coordinate of the excited magnetization, after a zero order phase correction.

Finally, in Fig. 5A, we taper the edges of chirp pulse so that we don't have to sweep very far. We choose peak Amplitude of last π pulse as 15 kHz, center π pulse as $\frac{15}{\sqrt{2}}$ kHz and $\frac{\pi}{2}$ pulse as 3 kHz. The Bandwidth $B/2\pi = 150$ kHz and $C/2\pi = 180$ kHz. Sweep rate $a = 2.7 \times (2\pi \times 3 \text{ kHz})^2$ and time $T = 2.36$ ms. Total duration of the pulse sequence is 7.07 ms. Fig. 5B, shows the x-coordinate of the excited

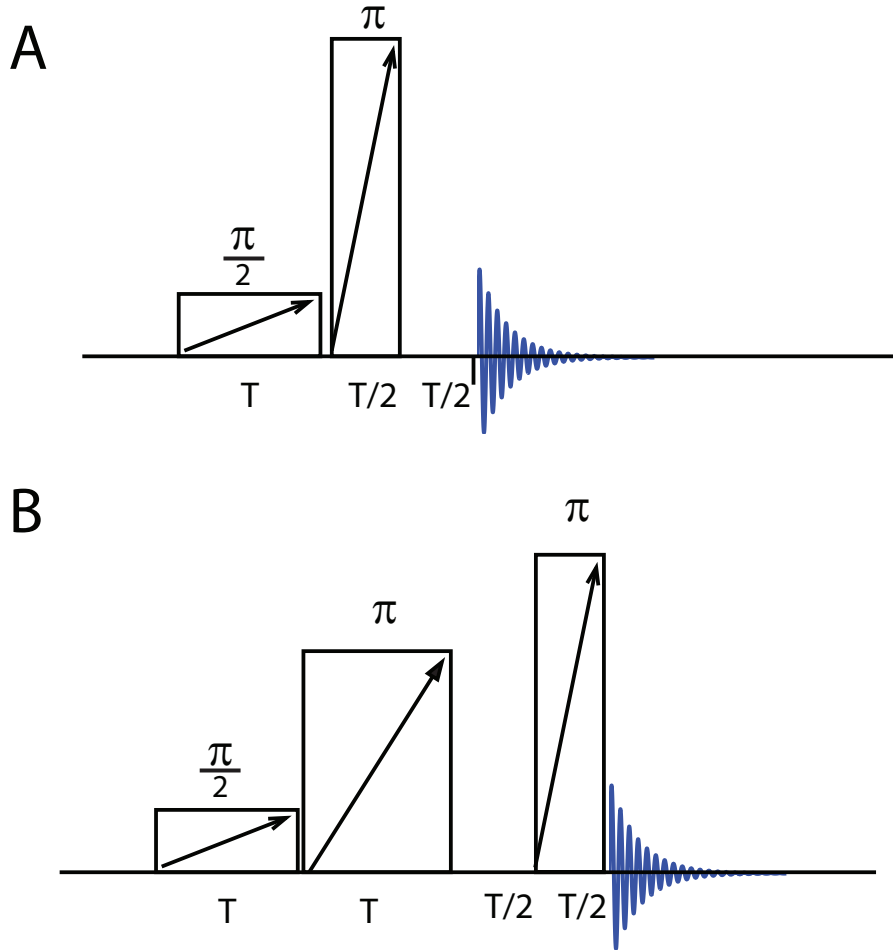


Figure 3: Fig. A shows the pulse sequence with a $\frac{\pi}{2}$ excitation pulse of duration T followed by a π inversion pulse of duration $\frac{T}{2}$ at twice the sweep rate and finally a free evolution for time $\frac{T}{2}$. Fig. B shows the pulse sequence with a $\frac{\pi}{2}$ excitation pulse of duration T followed by a π inversion pulse of duration T both at same sweep rate and finally a free evolution for time $\frac{T}{2}$ followed by a π inversion pulse of duration $\frac{T}{2}$ at twice the chirp rate. The ratio of amplitude of last π pulse to center π pulse is $\sqrt{2}$.

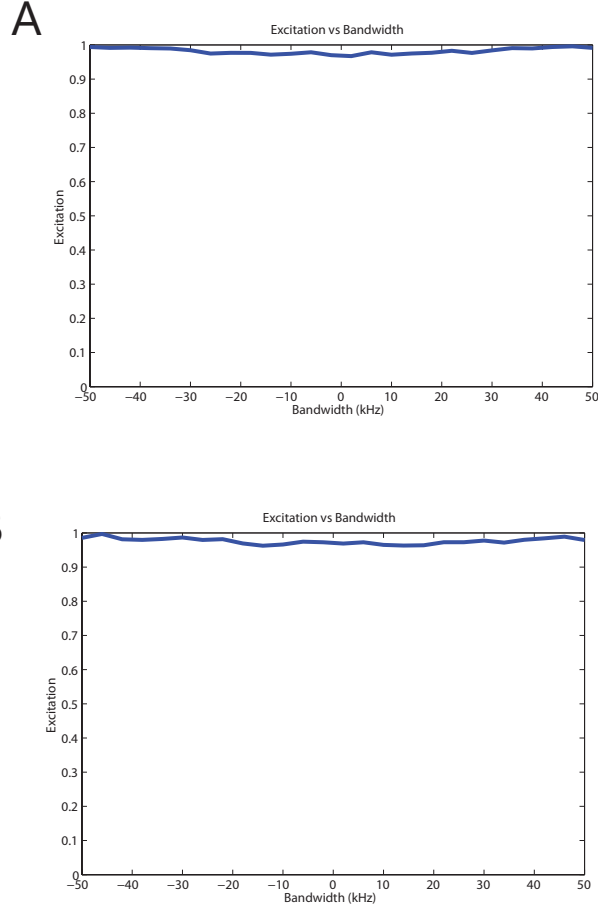


Figure 4: In Fig. A we choose amplitude of π pulse as 10 kHz and $\frac{\pi}{2}$ pulse as 1 kHz. The Bandwidth $B/2\pi = 50$ kHz and $C/2\pi = 400$ kHz. Sweep rate $a = 2.7 \times (2\pi \text{ kHz})^2$ and time $T = 47.15$ ms. Total duration of the pulse is 94.13 ms. In Fig. B we choose amplitude of last π pulse as 10 kHz, center π pulse as $\frac{10}{\sqrt{2}}$ kHz and $\frac{\pi}{2}$ pulse as 1 kHz. The Bandwidth $B/2\pi = 50$ kHz and $C/2\pi = 150$ kHz. Sweep rate $a = 2.7 \times (2\pi \text{ kHz})^2$ and time $T = 17.68$ ms. Total duration of the pulse is 53.0516 ms.

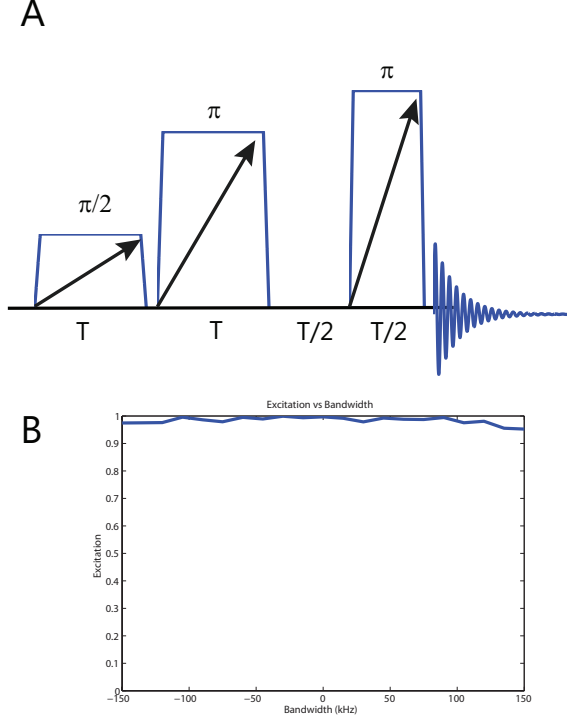


Figure 5: Fig. A shows the pulse sequence with a $\frac{\pi}{2}$ excitation pulse of duration T followed by a π inversion pulse of duration T both at same sweep rate and finally a free evolution for time $\frac{T}{2}$ followed by a π inversion pulse of duration $\frac{T}{2}$ at twice the chirp rate. The amplitude at ends of chirp pulses is tapered to minimize sweep width. The ratio of peak amplitude of last π pulse to center π pulse is $\sqrt{2}$. Fig. B shows the excitation profile after a zero order phase correction of the pulse sequence in Fig. A. We choose peak amplitude of last π pulse as 15 kHz, center π pulse as $\frac{15}{\sqrt{2}}$ kHz and $\frac{\pi}{2}$ pulse as 3 kHz. The bandwidth $B/2\pi = 150$ kHz and $C/2\pi = 180$ kHz. Sweep rate $a = 2.7 \times (2\pi \times 3 \text{ kHz})^2$ and time $T = 2.36$ ms. Total duration of the pulse sequence is 7.07 ms.

magnetization, after a zero order phase correction.

Experimental realization of this pulse sequence is done on a 750 MHz spectrometer. Fig. 6 shows experimental excitation profiles of residual HDO signal in a sample of 99.5% D_2O , as a function of resonance offset, after application of the pulse sequence in Fig. 5A. The offset is varied in increments of 6 kHz, over a range of 300 kHz ($[-150, 150]$ kHz) around the proton resonance at 4.7 ppm. The peak amplitude of the pulse is 15 kHz. We find uniform excitation experimentally.

This pulse sequence appears as CHORUS in [18]. Here we provide details of the

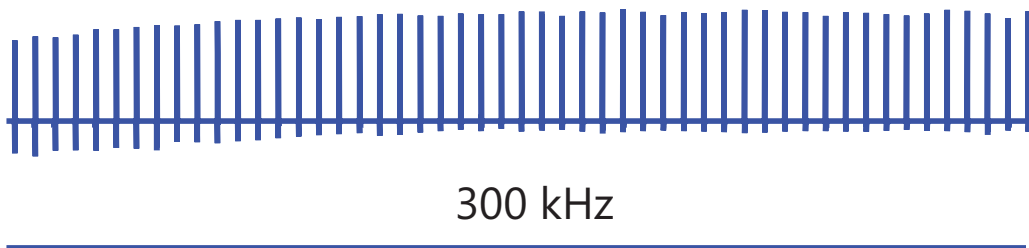


Figure 6: Above figure shows experimental excitation profiles of residual HDO signal in a sample of 99.5% D₂O, as a function of resonance offset, after application of the pulse sequence in Fig. 5A. The offset is varied in increments of 6 kHz, over a range of 300 kHz as in fig. 5B

working of this sequence.

4 Conclusion

In this paper we developed the theory of broadband chirp excitation pulses. We first developed a three stage model for understanding chirp excitation in NMR. We then showed how a chirp π pulse can be used to refocus the phase of the chirp excitation pulse. The resulting magnetization still had some phase dispersion in it. We then showed how a combination of two chirp π pulses instead of one can be used to eliminate this dispersion, leaving behind a small residual phase dispersion. The excitation pulse sequence presented here allow exciting arbitrary large bandwidths without increasing the peak rf-amplitude. They are expected to find immediate application in ¹⁹F NMR. Although methods presented in this paper have appeared elsewhere [7, 8, 18], we present complete analytical treatment that elucidates the working of these methods. Future work in direction is to use these methods to develop general purpose rotation pulses, like a broadband $(\frac{\pi}{2})_x$ rotation.

References

- [1] R. Freeman, S. P. Kempsell, M.H. Levitt, Radio frequency pulse sequence which compensate their own imperfections, J. Magn. reson. 38 (1980) 453-479.

- [2] M.H. Levitt, Symmetrical composite pulse sequences for NMR population inversion. I. Compensation of radiofrequency field inhomogeneity, *J. Magn. Reson.* 48 (1982) 234-264.
- [3] M.H. Levitt, R. R. Ernst, Composite pulses constructed by a recursive expansion procedure, *J. Magn. Reson.* 55(1983) 247-254
- [4] R. Tycho, H.M. Cho, E. Schneider, A. Pines, Composite Pulses without phase distortion, *J. Magn. Reson.* 61(1985)90-101.
- [5] M.H. Levitt, Composite Pulses, *Prog. Nucl. Magn. Reson. Spectrosc.* 18(1986) 61-122.
- [6] A.J. Shaka, A. Pines Symmetric phase-alternating composite pulses, *J. Magn. Reson.* 71(1987) 495-503.
- [7] J.-M. Böhlen, M. Rey, G. Bodenhausen, Refocusing with chirped pulses for broadband excitation without phase dispersion, *J. Magn. Reson.* 84 (1989) 191-197.
- [8] J.-M. Böhlen, G. Bodenhausen, Experimental aspects of chirp NMR spectroscopy, *J. Magn. Reson. Ser. A.* 102(1993)293-301.
- [9] D. Abramovich, S. Vega, Derivation of broadband and narrowband excitation pulses using the Floquet formalism, *J. Magn. Reson. Ser. A.* 105(1993)30-48.
- [10] E. Kupce, R. Freeman, Wideband excitation with polychromatic pulses, *J. Magn. Reson. Ser. A.* 108(1994) 268-273.
- [11] K. Hallenga, G. M. Lippens, A constant-time ^{13}C - ^1H HSQC with uniform excitation over the complete ^{13}C chemical shift range, *J. Biomol. NMR* 5(1995) 59-66.
- [12] T. L. Hwang, P.C.M van Zijl, M. Garwood, Broadband adiabatic refocusing without phase distortion, *J. Magn. Reson.* 124 (1997)250-254.
- [13] K.E. Cano, M.A. Smith, A.J. Shaka, adjustable, broadband, selective excitation with uniform phase, *J. Magn. Reson.* 155 (2002) 131-139.

- [14] J. Baum, R. Tycko, A. Pines, Broadband and adiabatic inversion of a two level system by phase modulated pulses, *Phys. rev. A.* 32 (1985) 3435-3447.
- [15] T.E. Skinner, T. O. Reiss, B. Luy, N. Khaneja, S. J. Glaser, Application of optimal control theory to the design of broadband excitation pulses for high-resolution NMR, *J. Magn. Reson.* 163 (2003) 8-15.
- [16] T. E. Skinner, K. Kobzar, B. Luy, M. R. Bendall, W. Bermel, N. Khaneja, and S. J. Glaser, Optimal control design of constant amplitude phase-modulated pulses: application to calibration-free broadband excitation, *Journal of Magnetic Resonance.* 179 (2006) 241.
- [17] K. Kobzar, T.E. Skinner, N. Khaneja, S. J. Glaser, B. Luy, Exploring the limits of broadband excitation and inversion:II. Rf-power optimized pulses, *J. Magn. Reson.*, 194(1), 58-66, (2008).
- [18] J. E. Power, M. Foroozandeh, R.W. Adams, M. Nilsson, S.R. Coombes, A.R. Phillips, G. A. Morris, Increasing the quantitative bandwidth of NMR measurements, DOI: 10.1039/c5cc10206e, *Chem. Commun.* (2016).
- [19] M.R.M. Koos, H. Feyrer, B. Luy, Broadband excitation pulses with variable RF amplitude-dependent flip angle (RADFA), *Magn. Reson. Chem.*, Vol. 53, Issue 11, pp 886-893, 2015.
- [20] N. Khaneja, A. Dubey, H.S. Atreya, Ultra broadband NMR spectroscopy using multiple rotating frame technique, *J. Magn. Reson.* 265(2016) 117-128.